Deactivation of Ceria-Based SOFC Anodes in Methanol

Taeyoon Kim, Kipyung Ahn, John M. Vohs, and Raymond J. Gorte
Department of Chemical & Biomolecular Engineering
University of Pennsylvania
Philadelphia, PA, 19104
gorte@seas.upenn.edu
Tel: (215) 898-4439
Fax: (215) 573-2093

Abstract

The performance and stability of Cu-ceria-YSZ (yttria-stabilized zirconia) and carbon-ceria-YSZ, solid-oxide-fuel-cell (SOFC) anodes were examined in neat (100%) methanol at 973 K and compared to the performance of the same anodes in dry H_2. The presence of Cu catalyzed the decomposition of methanol, so that the initial performance of cells with Cu-ceria-YSZ anodes was similar for methanol and H_2. However, with carbon-ceria-YSZ anodes, the open-circuit voltage was significantly higher and the reaction over-potential significantly lower in methanol than in H_2, suggesting that methanol is a more effective reductant of the anode three-phase boundary region. Carbon-ceria-YSZ anodes were found to undergo rapid and irreversible deactivation in methanol. Steady-state rates of methanol decomposition over ceria-YSZ were found to exhibit a similar deactivation the carbon-ceria anodes. Although no evidence for carbon deposition was observed with methanol at 973 K, the addition of steam was found to partially stabilize both anode and catalyst performance. SEM of ceria particles in YSZ showed a large change in the morphology of the ceria particles when the samples were heated in methanol, while negligible changes were observed when heating in H_2. It is suggested that the results with methanol can be explained as resulting from the very low $P(O_2)$ that is effectively produced by having methanol in contact with ceria.

Introduction

Methanol is an interesting fuel for fuel cells because it is a convenient way of storing chemical energy. While it is typically made from natural gas [1,2], it is much more easily stored than either natural gas or H_2 because it is a liquid at ambient conditions. It is also easily reformed back to CO and H_2 at relatively mild temperatures [3]. In solid oxide fuel cells (SOFC), methanol can be fed to the anode directly [4-8], even with Ni-based anodes and without reforming, since it carries sufficient oxygen to avoid entering into the thermodynamically unstable, carbon-forming regime [9].

However, there is an additional interesting aspect associated with using methanol in an SOFC. The reforming reaction, $CH_3OH = CO + 2H_2$, results in a significant loss in free energy due to the increase in entropy associated with forming three moles of product from each mole of methanol. This can be seen graphically in Fig. 1, which shows the Nernst potentials referenced to normal air for the following electrochemical reactions as a function of fuel utilization at 973 K:

$$CH_3OH + 1.5\ O^{2-} = CO_2 + 2H_2O + 3\ e^- \quad (1)$$

$$H_2 + 0.5\ O^{2-} = H_2O + 1\ e^- \quad (2)$$

$$CO + 0.5\ O^{2-} = CO_2 + 1\ e^- \quad (3)$$

If it were possible to electrochemically oxidize methanol, reversibly, a cell could achieve significantly higher open-circuit voltages (OCV) than are possible with CO or H_2. On a more practical level, the high Nernst potential corresponds to a very low $P(O_2)$, which implies that methanol is capable of producing a highly reducing environment that could affect components of the anode. For example, CeO_2, which is sometimes added to anode formulations to provide mixed conductivity and catalytic activity, has an equilibrium composition of $CeO_{1.97}$ (~6% of Ce atoms in the +3 oxidation state) at 973 K at the $P(O_2)$ established by equilibrium with humidified (3% H_2O) H_2 [10]. By comparison, equilibrium methanol oxidation, even at 50% fuel utilization, would result in a much lower $P(O_2)$ and lead to a more highly reduced state for ceria.

In the present study, we examine the performance of ceria-based anodes in methanol and show evidence that "over-reduction" of the ceria appears to have a deleterious impact on the morphology of the ceria and its catalytic activity.

Experimental

The fuel cells used in the present study were prepared by tape casting methods according to procedures described elsewhere [11,12]. First, a YSZ wafer, having a dense 60-μm thick layer

supported on a porous 600-μm thick layer, was fabricated by calcination of a two-layer green tape to 1823 K. The porosity of the 600-μm layer was approximately 65% and was obtained by including graphite and polystyrene pore formers in that part of the green tape. A 50:50 mixture of YSZ and LSM ($La_{0.8}Sr_{0.2}MnO_3$, Praxair Surface Technologies) powders was painted onto the dense side of the wafer and then heated in air to 1523 K to form the cathode. The active area of each cell, 0.35 cm^2, was defined by the area of the cathode. After calcination of the cathode, the anode components were added to the porous side of the YSZ wafer using wet impregnation of aqueous nitrate solutions, followed by calcination at 723 K to decompose the nitrate ions. Electrical contact with the cells was achieved using Ag paste and a Ag wire at the cathode and a Au wire with Au paste at the anode. On the anode side, the Au paste was only used to attach the Au wire and was not spread over the entire anode area. Finally, the cells were sealed onto1.2-cm alumina tubes using a zirconia-based adhesive (Aremco, Ceramabond 552) and placed inside a horizontal furnace.

Several anode compositions were tested. The standard Cu-ceria cell had 15-wt% ceria and 30-wt% Cu, with ceria added prior to the Cu. Because Cu is a good catalyst for methanol decomposition, anodes were also made with varying amounts of ceria but without Cu. To achieve electrical conductivity in these cells, the anodes were exposed to n-butane at 973 K for 4 h in order to deposit a layer of conductive carbon [13,14].

Cell performance was measured in both dry H_2 and neat (100%) CH_3OH at 973 K. While some moisture is always present at the anode due to leaks and internally generated water, we used dry H_2 for better comparison to neat methanol. Methanol was fed to the cells with a syringe pump at 0.5 ml/h, without dilution. To minimize gas-phase reactions, the tubes on which the cells were attached were placed only 3 cm into the furnace in order to minimize the pre-heat zone. The cell temperature was not affected by this cell placement, as demonstrated by the fact that the initial V-i polarization curves and the ohmic resistances (associated with the electrolyte) in the impedance spectra were unaffected by the placement of the cells or the length of the pre-heat zone. All impedance spectra were measured at a cell current density of 200 mA/cm^2 in the galvanostatic mode with a frequency range from 0.01 Hz to 100 kHz and a 1 mA AC perturbation, using a Gamry Instruments Potentiostat.

The methanol-decomposition reaction was characterized on catalysts that were similar to the fuel-cell anodes. These were prepared by impregnating either 20-wt% ceria or a mixture of

18-wt% ceria and 10-wt% Cu into a porous YSZ slab made from the same slurry used for tape casting the porous layer in the fuel cell. The amount of catalyst used in these studies, 75 mg, was also similar to the anode mass in the fuel cell. The reactions were characterized in a quartz-tube flow reactor, using an on-line gas chromatograph (Buck Scientific, model 8610) to determine methanol conversion. Methanol was supplied to the reactor by flowing He through a packed bed filled with methanol at 298 K.

Scanning electron microscopy (SEM, FEI DB235 FIB) was used to characterize the morphology of CeO_2 particles on YSZ porous matrices after exposure to various gas-phase environments.

Results

Because Cu is an excellent catalyst for methanol synthesis and methanol decomposition [15-17], its presence in the anode significantly influences cell performance in methanol. This is shown in Fig. 2. Fig. 2a) provides the V-i polarization curves at 973 K for a cell having an anode with 30-wt% Cu and 15-wt% ceria in dry H_2 and neat methanol. The cell performance is almost indistinguishable in the two fuels suggesting that methanol decomposes to CO and H_2 on the Cu anode prior to reaching the electrolyte interface. The results for the anode with 20-wt% ceria but using carbon for electronic conduction are quite different. The OCV in methanol was 1.24 V, compared to 1.15 V in dry H_2, and polarization losses with methanol were much lower than with H_2. As will be shown later, ceria is a catalyst for methanol decomposition, even though it is not as active as Cu; therefore, the low OCV for methanol compared to the theoretical Nernst potential, may be due to the fuel at the anode containing a mixture of CH_3OH, CO and H_2. Alternatively, irreversibility of the methanol-oxidation reaction may lead to a lower OCV [18]. Whatever the explanation, it is apparent that neat methanol establishes a lower $P(O_2)$ and provides a lower reaction overpotential at the anode three-phase boundary than does dry H_2.

The impedance spectra corresponding to the data in Fig. 2b) are shown in Fig. 3. For both fuels, the ohmic resistance of the cell, determined from the high-frequency intercept with the abscissa in the Cole-Cole plot, was 0.6 $\Omega \cdot cm^2$. This value is primarily associated with the YSZ electrolyte, but also has a contribution from the carbon anode. Because the Au paste used for current collection covered only a fraction of the anode surface, poor lateral conductivity increased the observed ohmic resistance. In methanol, the non-ohmic component of the cell impedance, ~0.5 $\Omega \cdot cm^2$, contains a contribution from the LSM-YSZ cathode, which we have

earlier determined to be approximately 0.4 $\Omega \cdot cm^2$ [19,20]. Therefore, the polarization losses for the anode operating in methanol must be very small, ~0.1 $\Omega \cdot cm^2$. In contrast, the anode polarization loss for this same cell operating in dry H_2 is almost 1.0 $\Omega \cdot cm^2$. This dramatic difference must be due to methanol being more effective than H_2 as a reducing agent for ceria.

Unfortunately, the performance of the carbon-ceria anode in neat methanol was not stable. Fig. 4a) shows the V-i polarization curves in dry H_2 and neat methanol for the same carbon-ceria cell after exposure to neat methanol for 40 h. After this treatment, the OCV in methanol had dropped to 1.10 V and the maximum power density to 120 mW/cm^2. The corresponding impedance spectrum in Fig. 4b) shows that ohmic losses in methanol were unchanged but the non-ohmic losses increased dramatically, to almost 2.0 $\Omega \cdot cm^2$. The cell performance in dry H_2 also decreased. The OCV remained at 1.12 V but the maximum power density dropped to approximately 90 mW/cm^2. The impedance spectrum in H_2 showed a surprising increase in the ohmic resistance of the cell to 1.0 $\Omega \cdot cm^2$. Because the increased ohmic resistance could indicate a loss of carbon, we attempted to restore the cell performance by exposing the anode to n-butane for an additional 4 h; but this treatment did not restore either the ohmic resistance or the power density in dry H_2. Re-oxidation of the anode in air, followed by treatment in n-butane, also had minimal effect on the cell performance.

The deactivation of carbon-ceria anodes in neat methanol at 973 K was measured as a function of ceria content, with results shown in Fig. 5. In this figure, the power density at 0.5 V is plotted as a function of time for anodes with 10, 20, and 30-wt% ceria. Deactivation of the cell with 10-wt% ceria occurred almost immediately, while the cell with 20-wt% ceria was relatively stable for 10 h. For 30-wt% ceria, the cell performance improved during the first day before also undergoing deactivation. Fig. 6 shows the results of a similar stability test on a cell with anode composed of 30-wt% Cu and 15-wt% ceria. The cell was initially tested for 120 h in a 2:1 mixture of H_2 and CO and an additional 48 h in CO to demonstrate that it was stable in the products that would be formed by decomposition of methanol. However, when the fuel to the cell was switched to neat methanol, the power density slowly declined. This result suggests that the Cu converts most of the methanol to syngas before it reaches the electrolyte interface, thereby slowing but not eliminating the deactivation process observed on the fuels with carbon-based anodes.

The loss in cell performance in neat methanol appears to be partially related to changes in catalytic activity of ceria. Fig. 7 displays a plot of the conversion of methanol over a porous YSZ slab with either 20-wt% ceria or 18-wt% ceria and 10-wt% Cu. In the absence of a catalyst, the methanol conversion was 15%, due to thermally induced reactions and reactions on the reactor walls. In all cases, the primary products of the reaction were H_2 and CO, although trace amounts of CO_2 and formaldehyde were also observed. The data in Fig. 7 indicate that ceria-YSZ exhibits high activity for the conversion of methanol initially, but the activity of the ceria-YSZ sample dropped precipitously after 5 h. The Cu-ceria-YSZ sample also deactivated with time but the deactivation was not as precipitous. Based on weight measurements of the catalyst samples following reaction, carbon formation with methanol was negligible in each case. Also, there was no evidence for bulk formation of carbonates [21], which can form on reduced ceria but likely decompose at this high temperature. While we are not aware of previous deactivation studies for ceria decomposing on ceria, there is a previous literature report showing high activity for methanol composition on ceria in the absence of steam, without carbon formation, between 973 and 1273 K [22].

Interestingly, Fig. 7 also indicates that the addition of small amounts of steam, a H_2O:CH_3OH mole ratio of only 0.16, completely stabilized methanol conversion over the ceria-YSZ catalyst. To determine whether the addition of steam would stabilize fuel-cell performance, the power density at 0.5 V for a cell with a Cu-ceria-YSZ anode was measured as a function of time, similar to the experiment in Fig. 6, but the fuel stream was switched to a mixture of methanol and steam (H_2O:CH_3OH = 0.5) for 24 h in the middle of the test. Cell performance stabilized during the period in which steam was added and deactivation recommenced when the steam was removed. Because steam reacts with carbon at 973 K in the presence of ceria [23], this experiment could unfortunately not be performed with the carbon-ceria anodes, where the deactivation was more dramatic. Since there was no evidence for carbon formation with methanol in any of these experiments, the effect of adding water is likely that of lowering the $P(O_2)$.

In an attempt to understand how the methanol affects the anodes, scanning electron micrographs of a porous YSZ wafer containing 20-wt% ceria were collected after various pretreatments. Because the porous YSZ has been calcined to 1823 K, its surface is smooth and featureless, as images in previous studies have already shown [24]. Fig. 8a) is the micrograph

obtained immediately following addition of the $Ce(NO_3)_3$ salts and calcination in air at 973 K for 24 h. The ceria forms a layer of small particles, ranging in size from 20 to 40 nm, covering the YSZ pores. Fig. 8b) demonstrates that reducing the sample in dry H_2 at 973 K for 48 h does not cause any significant change. The ceria particles remain similar in size and continue to cover the YSZ pores in a continuous, connected manner. However, dramatic changes in the ceria film occurred when the sample was treated in neat methanol at 973 K for 48 h, as shown in the image in Fig. 8c). Exposing the ceria to methanol caused significant growth of the ceria particles to diameters greater than 50 nm. Furthermore, while the ceria particles on the samples treated in air or H_2 appear to be in physical contact with neighboring particles, the ceria particles in Fig. 8c) have formed isolated islands.

The change in morphology of the ceria within the pores upon treatment in methanol can explain several observations in the fuel-cell deactivation. Clearly, the contact between the ceria and the YSZ pores is much worse in Fig. 8c), causing a decrease in the ceria surface area for reaction of methanol and a decrease in the area for oxygen exchange between ceria and the YSZ. The fact that the ceria particles after methanol exposure are no longer in contact with each other is probably responsible for the increased ohmic resistance observed on deactivated cells operating in H_2 (e.g. Fig. 4b)). A previous study of impregnated electrodes found that cells made without ceria exhibited higher ohmic resistances [25], implying that ceria helps provide electronic conductivity along the pore walls. Obviously, if contact between particles is lost, ceria cannot assist in current collection. Questions still remain regarding why the ohmic resistances are different when the measurements were performed in H_2 and in methanol. Perhaps methanol is such an effect reducing agent that the YSZ surface is also reduced in methanol [26].

Discussion

There are several surprising observations arising from the results in this study. First, the very low anode polarization losses observed with methanol on the carbon-ceria anodes, at least during the initial exposures to methanol, demonstrate that methanol can be more effective than H_2 at reducing ceria. Reduction by hydrogen requires dissociation of the H-H bond, a process that occurs readily over transition metals but is much more difficult over oxides like ceria. Indeed, that dissociation of H_2 limits reaction on ceria-based anodes is demonstrated by the fact that the addition of dopant levels of precious-metal catalyst to ceria significantly improves the performance of these electrodes [18]. Because oxides are highly polar, they readily break the

H_3C-OH bond of methanol in the absence of any additional catalyst. Indeed, there are indications that fully oxidized ceria is able to catalyze the reaction of methanol at temperatures as low as 200 K [27]. Once this dissociation occurs, reduction of the oxide occurs rapidly.

The second surprise is the large change in ceria morphology that occurs upon treatment of ceria at a temperature of only 973 K. That macroscopic movement of ceria in contact with YSZ can occur following oxidation and reduction has already been demonstrated with ceria films on YSZ single crystals [28,29], but this movement has not previously been reported to affect fuel-cell properties. Furthermore, the previous work with ceria films on YSZ found that reduction caused ceria to "spread" over the YSZ surface, the opposite of what appears to be occurring to ceria upon methanol exposure in the fuel cell. Since the thin-film studies found the morphology of ceria films depended on the nature of the substrate, with ceria films behaving very differently on YSZ and α-Al_2O_3 surfaces [28,29], the changes in the ceria morphology are driven at least in part by ceria-YSZ interfacial energies. The importance of this conclusion is that it may be possible to prevent migration of the ceria by tailoring the nature of the oxide-oxide interaction. For example, a study from our laboratory has shown that ceria in the SOFC anode can be replaced by a ceria-zirconia, solid solution with minimal effect on fuel-cell performance [30]. One would expect the interfacial energies to be very different for YSZ with ceria and with the solid solution.

Finally, the treatment of ceria in methanol seems to affect the catalytic properties of ceria, in addition to the morphology of the ceria films. The drop in the reaction rate for methanol decomposition over ceria is too large to explain as being the result simply of changes in ceria surface area. Again, the catalyst literature may provide clues as to what is happening. It has been reported that the catalytic activity of ceria depends on its history [31-33], although the physical reasons for this are still not known. One possibility is that small ceria crystallites have thermodynamic properties different from bulk ceria. Indeed, it has been reported that the enthalpy of oxidation on reduced ceria nanoparticles is approximately half the enthalpy of oxidation for bulk ceria [34]. Another possibility is that surface interactions with a support could change ceria reducibility. Again, there are reports in the literature indicating ceria in contact with zirconia is much easier to reduce than bulk ceria [35]. The morphology changes that occur following methanol treatment clearly do affect the contact between ceria and the YSZ.

The discussion here has focused on the influence of methanol treatment with impregnated, ceria-based electrodes. However, the present results could well be important for more conventional fuel-cell designs as well. For example, it is common practice to use ceria interlayers to prevent solid-state reactions between components in SOFC. For ceria to be an effective interlayer, mobility must be suppressed. Understanding and controlling this mobility becomes a critical issue, which clearly deserves more study.

Conclusions

This study has shown that methanol is more easily oxidized than H_2 on ceria-based anodes, exhibiting large OCV and lower reaction over-potentials. Unfortunately, treating ceria in neat methanol causes changes in both the ceria morphology and catalytic activity, possibly due to the low effective $P(O_2)$ that is established. Finally, the results highlight the fact that species within SOFC electrodes can be very mobile, even at relatively low temperatures.

Acknowledgement

This work was supported by the Office of Naval Research.

References:

1. A. Cybulski, Catal. Rev. Sci. Eng., 36 (1994) 557.

2. Kirk-Othmer, Encyclopedia of Chemical Technology, 4th Edition (1995).

3. P. J. de Wild and M. J. F. M. Verhaak, Catal. Today, 60 (2000) 3.

4. Y. Jiang and A. V. Virkar, J. Electrochem. Soc., 148 (2001) A706.

5. G. J. Saunders, J. Preece and K. Kendall, J. Power Sources,131 (2004) 23.

6. M. Sahibzada, B. C. H. Steele, K. Hellgardt, D. Barth, A. Effendi, D. Mantzavinos, I. S. Metcalfe, Chem. Eng. Sci., 55 (2000) 3077.

7. B. Feng, C. Y. Wang, and B. Zhu, Electrochem. & Sol. State Lett., 9 (2006) A80.

8. D. J. L. Brett, A. Atkinson, D. Cumming, E. Ramirez-Cabrera, R. Rudkin, N. P. Brandon, Chem. Eng. Sci., 60 (2005) 5649.

9. K. Sasaki, H. Kojo, Y. Hori, R. Kikuchi, and K. Eguchi, Electrochemistry 70 (2002) 18.

10. T. Kim, J. M. Vohs, and R. J. Gorte, Ind. Eng. Chem. Res. (2006), in press.

11. S. Park, R. J. Gorte, and J. M. Vohs, J. Electrochem. Soc., 148 (2001) A443

12. R. J. Gorte, S. Park, J. M. Vohs, and C. H. Wang, Adv. Mater., 12 (2000) 1465.

13. H. Kim, C. Lu, W. L. Worrell, J. M. Vohs, and R. J. Gorte, J. Electrochem. Soc.,149 (2002) A247.

14. S. McIntosh, J. M. Vohs, and R. J. Gorte, J. Electrochem. Soc., 150 (2003) A470.

15. M. Manzoli, A. Chiorino, and F. Boccuzzi, Appl. Catal. B 57 (2005) 201.

16. T. Tsoncheva, S. Vankova, O. Bozhkov, and D. Mehandjiev, J. Mol. Cat. A 225 (2005) 245.

17. X.M. Liu, G.Q. Lu, Z.F. Yan, and J. Beltramini, Ind. Eng. Chem. Res. 42 (2003) 6518.

18. S. McIntosh, J. M. Vohs, and R. J. Gorte, Electrochem. Solid-State Lett., 6 (2003) A240.

19. Y. Y. Huang, J. M. Vohs, and R. J. Gorte, J. Electrochem. Soc., 152 (2005) A1347.

20. S. McIntosh, S. B. Adler, J. M. Vohs, and R. J. Gorte, Electrochem. & Solid State Lett., 7 (2004) A111.

21. S. Sharma, S. Hilaire, J.M. Vohs, R.J. Gorte, and H.-W. Jen, Journal of Catalysis, 190 (2000) 199.

22. N. Laosiripojana and S. Assabumrungrat, Chem. Eng. Sci., 61 (2006) 2540.

23. T. Kim, G. Liu, M. Boaro, S. I. Lee, J. M. Vohs, R. J. Gorte, O. H. Al-Madhi, and B. O. Dabbousi, J. Power Sources, 155 (2006) 231.

24. H. He, Y. Huang, J. Regal, M. Boaro, J. M. Vohs, and R. J. Gorte, J. Am. Ceram. Soc., 87 (2004) 331.

25. O. Costa-Nunes, R. J. Gorte, and J. M. Vohs, J. Power Sources, 141 (2005) 241.

26. J. Zhu, J.G. van Ommen, H.J.M. Bouwmeester and L. Lefferts, J. Catal., 233 (2005) 434.

27. D. R. Mullin, M. D. Robbins, J. Zhou, Surf. Sci., 600 (2006) 1547.

28. O. Costa-Nunes, R. J. Gorte, and J. M. Vohs, J. Mater. Chem., 15 (2005) 1520.

29. O. Costa-Nunes, R. M. Ferrizz, R. J. Gorte, and J. M. Vohs, Surf. Sci., 592 (2005) 8.

30. K. Ahn, H. P. He, J. M. Vohs, and R. J. Gorte, Electrochem. & Solid-State Lett., 8 (2005) A414.

31. H. Cordatos, T. Bunluesin, J. Stubenrauch, J. M. Vohs, and R. J. Gorte, Journal of Physical Chemistry, 100 (1996) 785.

32. T. Bunluesin, R.J. Gorte, and G.W. Graham, Applied Catalysis B, 14 (1997) 105.

33. T. Bunluesin, R.J. Gorte, and G.W. Graham, Applied Catalysis B, 15 (1998) 107.

34. Y.-M. Chiang, E. B. Lavik, I. Kosacki, H. L. Tuller, J. Y. Ying, Appl. Phys. Lett, 69 (1996) 187.

35. E.S. Putna, T. Bunluesin, X.L. Fan, R.J. Gorte, J.M. Vohs, R.E. Lakis, and T. Egami, Catalysis Today, 50 (1999) 343

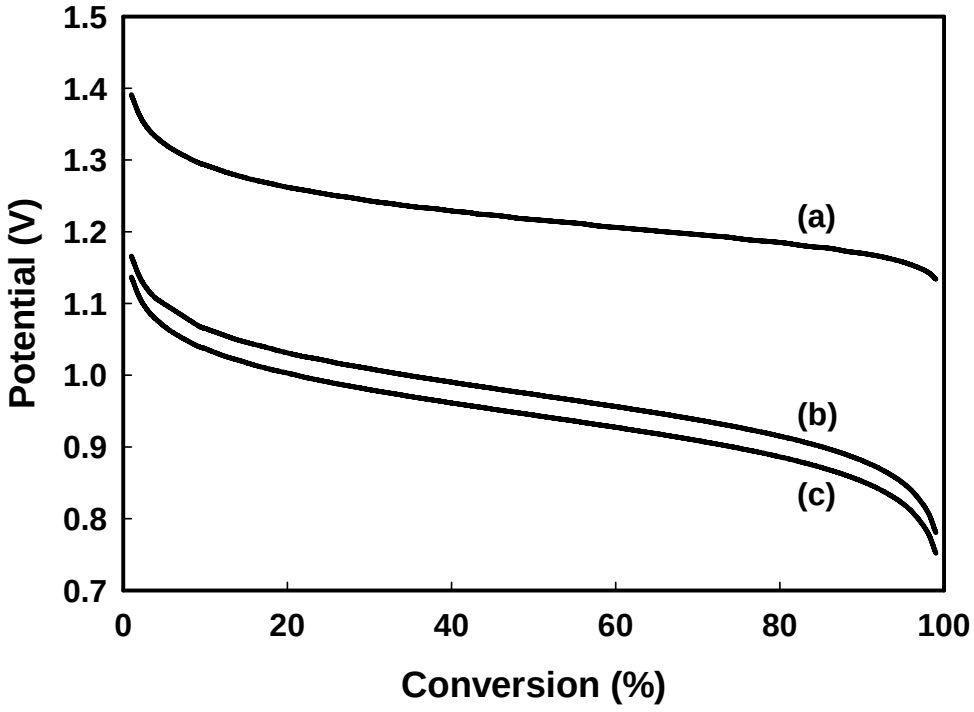

Figure 1. Nernst potentials at 973 K as a function of conversion for total oxidation of (a) methanol, (b) hydrogen, and (c) carbon monoxide.

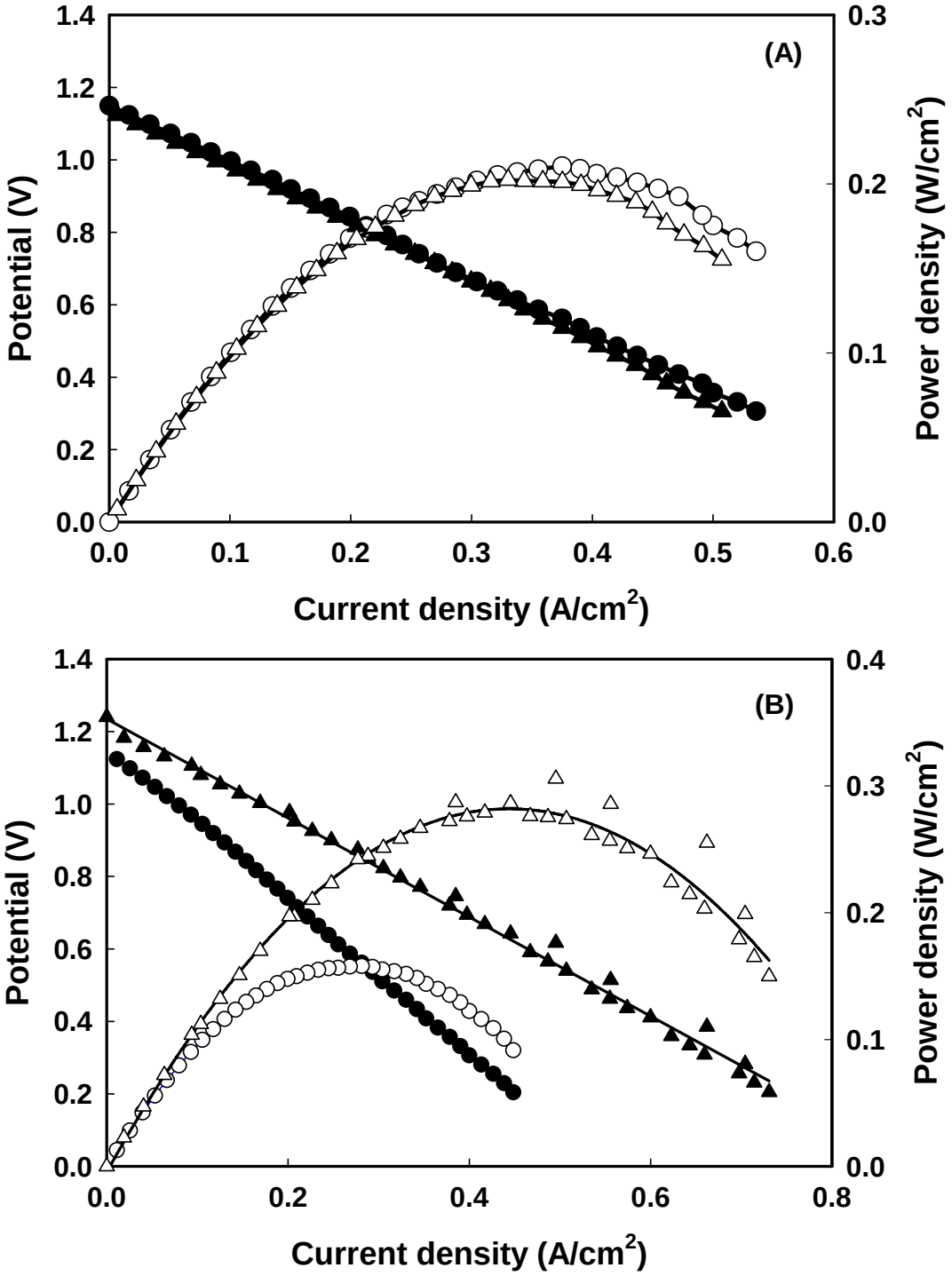

Figure 2. Initial V-i polarization curves for cells with (A) Cu-ceria-YSZ anodes and (B) carbon-ceria-YSZ anodes at 973 K in dry H_2 (●) H_2 and methanol (▲).

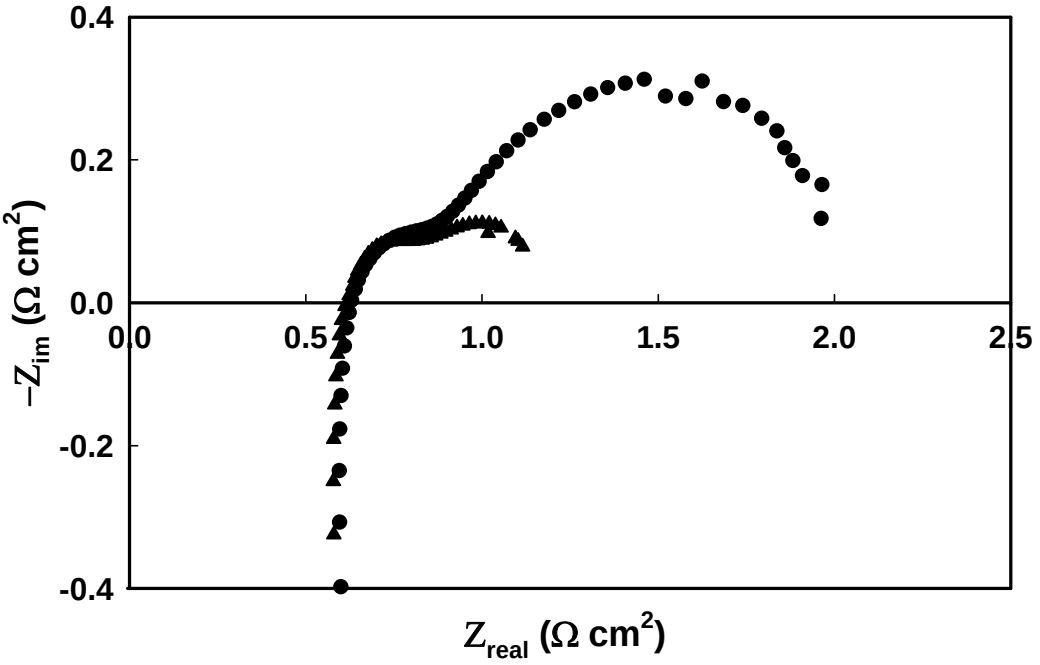

Figure 3. Cole-Cole plots for the cell in Fig. 2(B) at 973 K in H_2 (●) and methanol (▲).

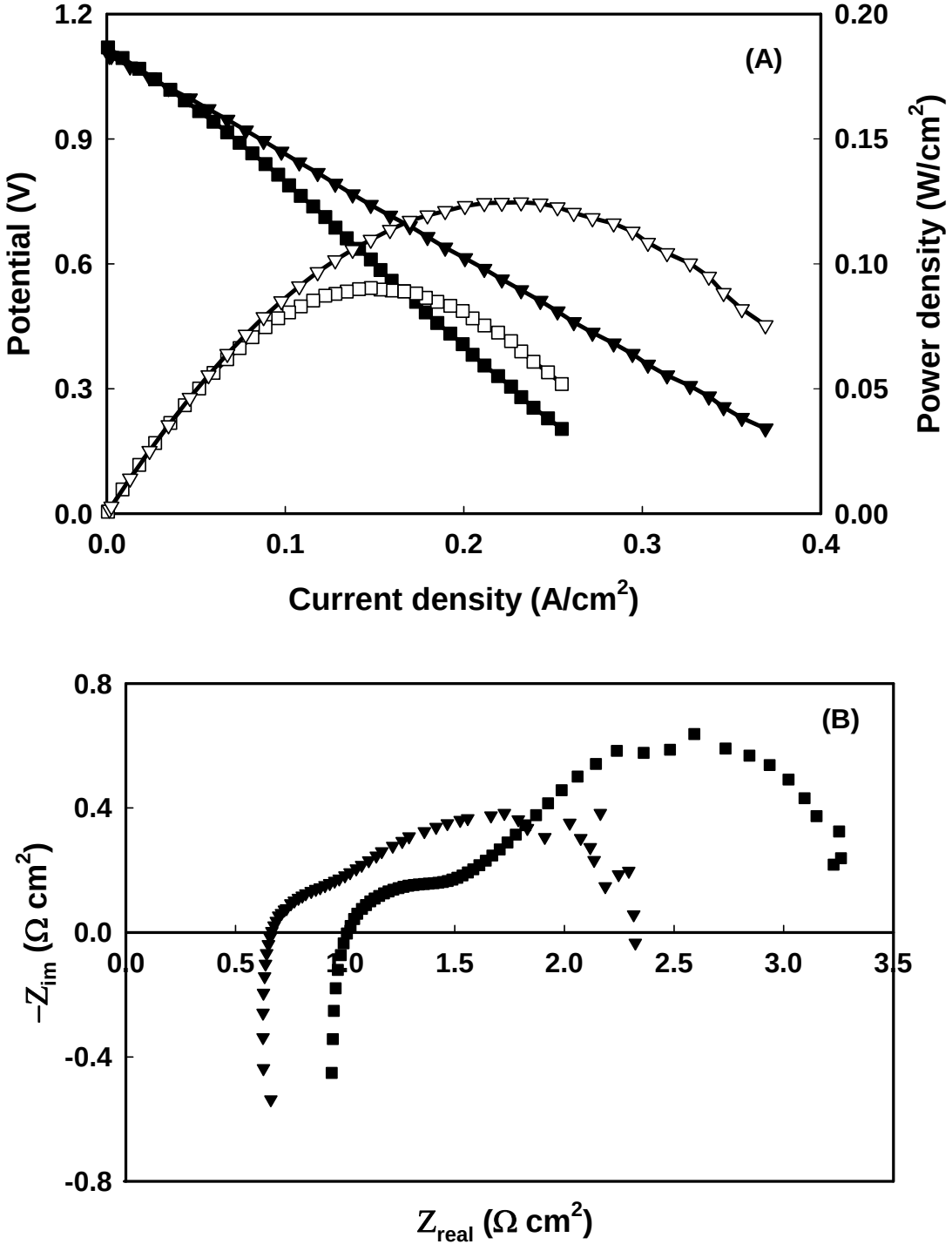

Figure 4. V-i polarization curves (A) and Cole-Cole plots (B) for the same cell as in Fig. 2(B) after deactivation by exposure to methanol at 973 K for 40 h. The data are for measurements in H_2 (■) and methanol (▼).

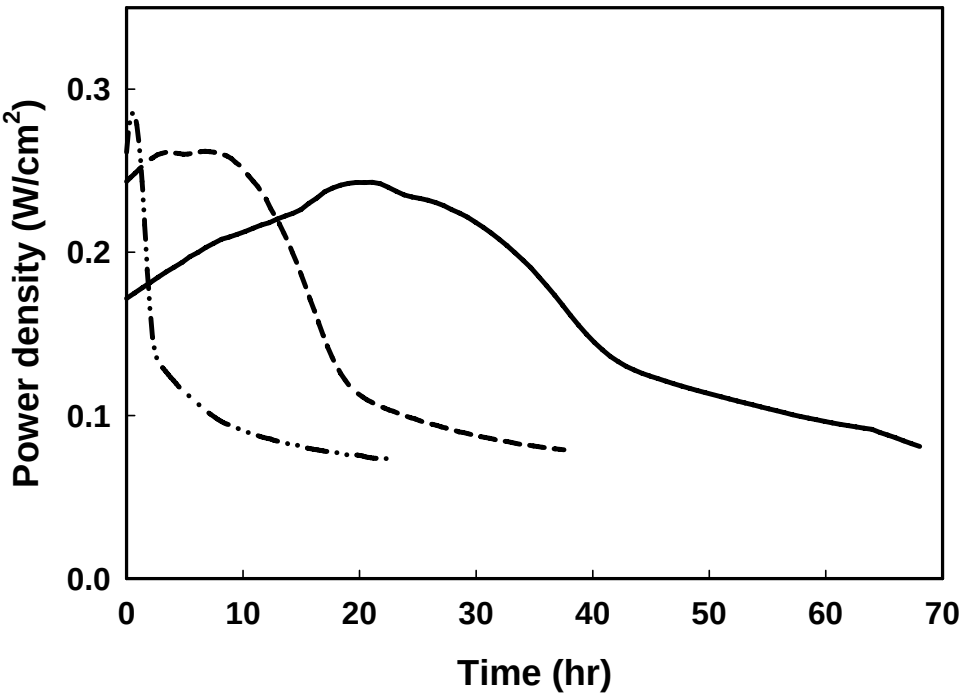

Figure 5. Power density at 973 K and 0.5 V for cells having carbon-ceria-YSZ anodes but different loadings of ceria: (–••–) 10wt%, (– – –) 20wt%, and (——) 30wt% CeO_2.

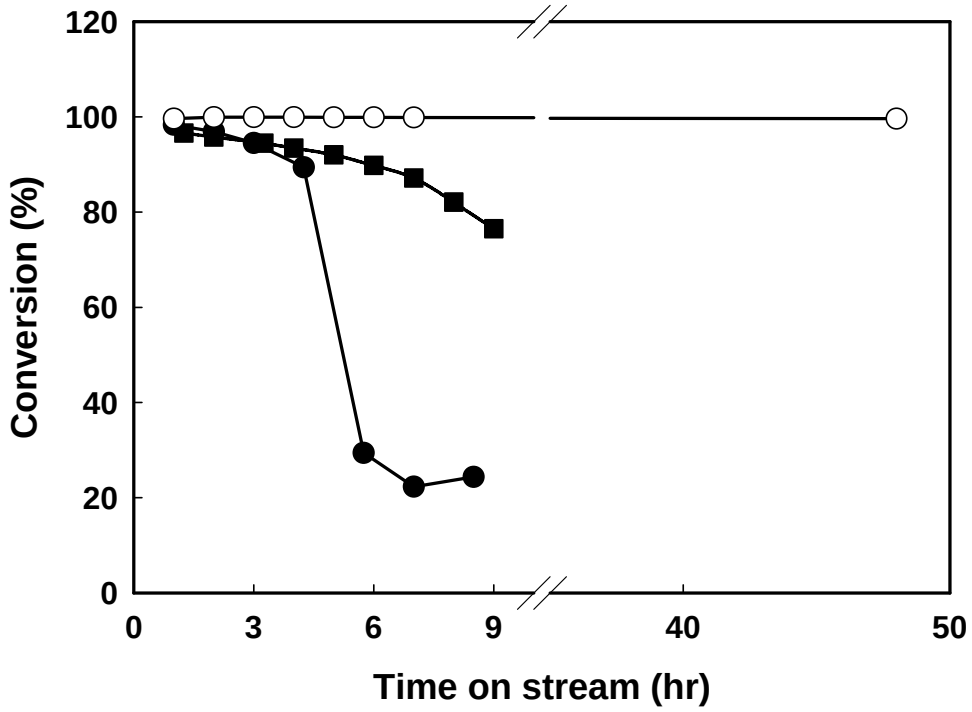

Figure 6. Methanol conversion as a function of time in a tubular reactor at 973 K over (–●–) ceria-YSZ and Cu-ceria-YSZ (–■–). The addition of steam (S/C = 0.16) significantly improved the stability of the ceria-YSZ catalyst (–○–).

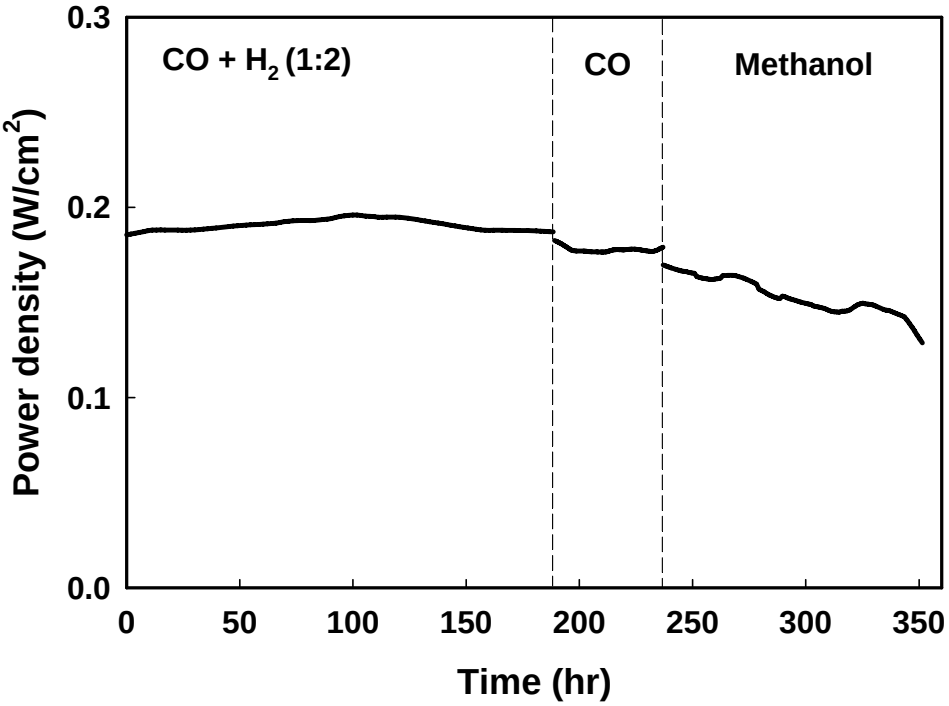

Figure 7. Power density at 973 K and 0.5 V for a cell having a Cu-ceria-YSZ anode in syngas (H_2 and CO in a 2:1 molar ratio), pure CO, and methanol.

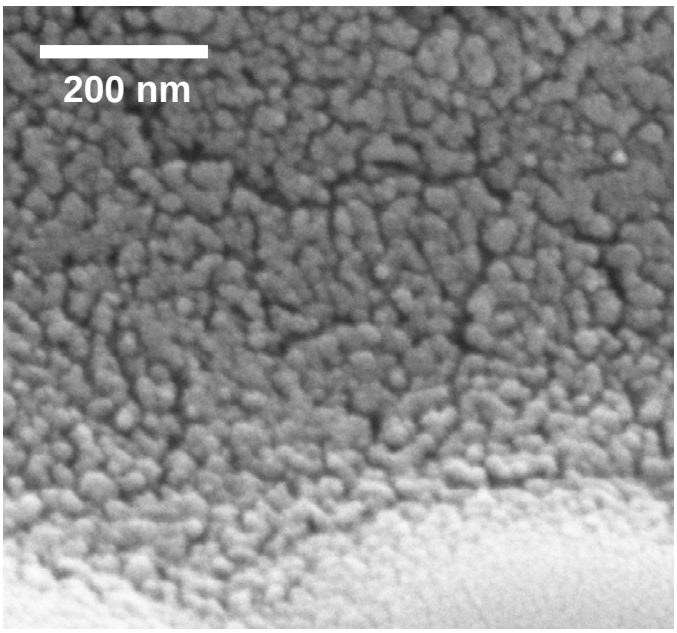

(A)

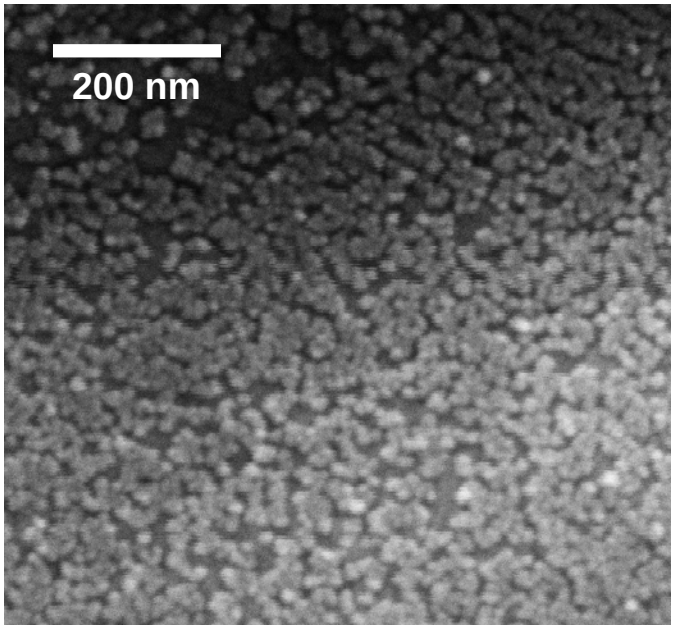

(B)

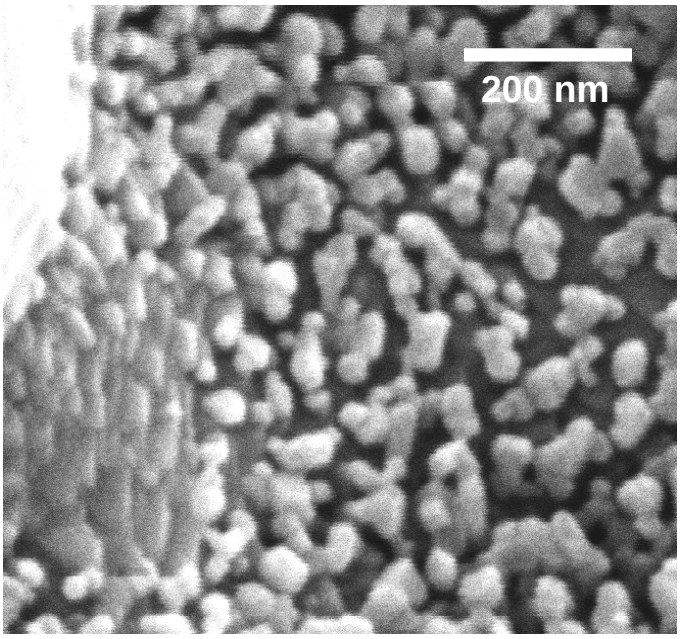

Figure 8. SEM micrographs of ceria-YSZ: (A) calcined in air at 973 K for 24 h; (B) heated in H_2 at 973 K for 48 h; and (C) heated in neat methanol for 48 h.